

Plenum Chamber Effect on Wind-Tunnel Resonance by the Finite-Element Method

In Lee*

Stanford University, Stanford, California

A finite-element approach is developed for predicting the so-called "resonant" frequencies of subsonic wind tunnels with plenum chambers. The resulting computer code has been applied to various wind tunnels. For example, the resonant frequencies for both the rectangular wind tunnel (rectangular cross section) and the NASA Langley Research Center 16 × 16 ft Transonic Dynamics Tunnel (octagonal cross section) have been calculated. Plenum chamber effects on wind-tunnel resonance is significant in a Mach number range of 0–0.5. The results are more accurate than theoretical values obtained by using an averaged homogeneous boundary condition on the slot.

Nomenclature

a_0	= speed of sound of fluid medium
a_e	= effective speed of sound of fluid medium defined in Eq. (15)
$[B]$	= matrix defined in Eq. (43)
b	= depth of plenum chamber
F	= variational functional for complementary system
$\{f\}$	= column vector on slot boundary defined in Eq. (44)
H	= height of tunnel
i	= $\sqrt{-1}$
$[K]$	= stiffness matrix for whole system
$[k]$	= element stiffness matrix
M	= freestream Mach number
$[m]$	= element mass matrix
$[M]$	= mass matrix for whole system
$[N]$	= row matrix of shape function
p	= perturbation pressure
$\{p\}$	= column vector of nodal pressure values
S	= boundary surface
t	= time
U	= freestream velocity
x, y, z	= rectangular coordinates
α	= wave number
β	= $\sqrt{1 - M^2}$
ξ	= acoustic displacement
ρ	= density in undisturbed stream, mean density
ϕ	= perturbation velocity potential in test section
ψ	= perturbation velocity potential in plenum chamber
ω	= angular frequency

I. Introduction

THE dynamic experimental test results in a wind tunnel may be affected by the so-called "resonance" problem when the model frequency is near a wind-tunnel resonant frequency. Runyan et al.¹ conducted experimental tests for the investigation of the tunnel resonance on the forces on an oscillating airfoil. Widmayer et al.² conducted some ex-

periments to measure the oscillatory aerodynamic forces and moments acting on a rectangular wing. The test results were in considerable error near the tunnel resonant frequency. The probable occurrence of resonance was also observed in experiments on the two-dimensional wing by Clevenson and Widmayer.³ There is, therefore, a need to be able to predict the wind-tunnel resonant frequency accurately.

The previous investigators^{4–7} have obtained the resonant frequencies based on the assumption that the plenum chamber surrounding the test section is large. However, the depth of the plenum chamber is generally less than twice the height of the test section. Therefore, the effect of the plenum chamber on the resonance should be considered. Mabey⁸ suggested that any theory that does not consider the plenum chamber effects for a slotted tunnel is in error in a Mach number range of 0–0.5. Mabey developed an improved theory applicable to wind tunnels that have finite plenum chambers, and this theory agrees well with experiments for rectangular tunnels. However, it is difficult to analyze the resonance for an arbitrarily shaped test section and plenum chamber. In this analysis, we will apply the finite-element method to this problem.

II. Governing Equation and Boundary Conditions

The cross section of a wind tunnel with a plenum chamber is shown in Fig. 1, and the side view of the wind tunnel is given in Fig. 2. We assume that the wind tunnel extends from $z = -\infty$ to $+\infty$ and has a uniform velocity U and a Mach number M . The test section height is H , and the plenum chamber depth is b . The wind tunnel has slotted walls between the test section and the plenum chambers, which are assumed to be thin and rigid and to have no viscosity effect. Furthermore, the mean pressure and static temperature are assumed to be the same in the test section and the plenum chambers. The densities in the test section and the plenum chambers are the same.

We denote the velocity potential in the test section as ϕ and in the plenum chamber as ψ . If we consider a rectangular coordinate system defined as shown in Figs. 1 and 2, then for small disturbances, the perturbation velocity potential in the test section satisfies the following equation:

$$(1 - M^2)\phi_{zz} + \phi_{xx} + \phi_{yy} - \frac{2M^2}{U}\phi_{zt} - \frac{M^2}{U^2}\phi_{tt} = 0 \quad (1)$$

Many wind tunnels have a number of slots running parallel to the axis of the tunnel to reduce the model blockage effect.

Presented as Paper 86-0898 at the AIAA/ASME/ASCE/AHS 27th Structures, Structural Dynamics, and Materials Conference, San Antonio, TX, May 19–21, 1986; received April 9, 1987; revision received Feb. 1, 1988. Copyright © 1986 by In Lee. Published by the American Institute of Aeronautics and Astronautics, Inc., with permission.

*Graduate student; currently Assistant Professor, Department of Mechanical Engineering, Korea Advanced Institute of Science and Technology. Member AIAA.

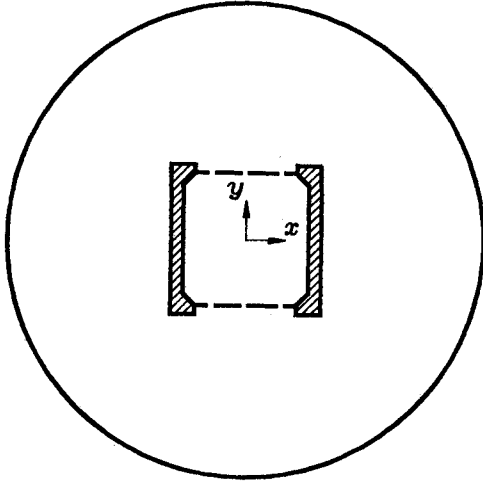


Fig. 1 Cross section of wind tunnel with plenum chamber.

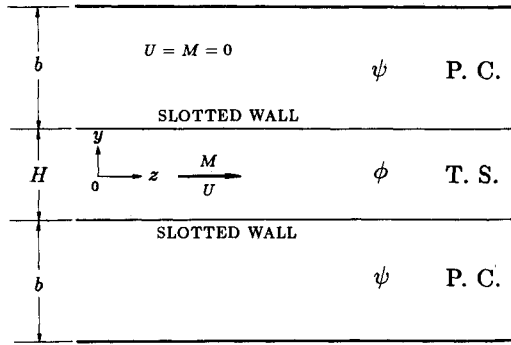


Fig. 2 Side view of wind tunnel with plenum chamber.

The boundary condition at a solid wall of the test section is $\partial\phi/\partial n = 0$. The flow in the absence of a model is given by $\phi = 0$ everywhere. However, it is necessary to obtain nonzero oscillatory solutions of Eq. (1) satisfying the same boundary conditions in order to solve the resonance problem.

For the test section, we assume disturbances of the form

$$\phi = \phi_R = \Phi(x, y) e^{i\alpha z} e^{i\omega t} \quad (2)$$

where Φ is any function of x and y and α is a streamwise wave number. Substituting Eq. (2) into Eq. (1), we get

$$\Phi_{xx} + \Phi_{yy} + \left[\frac{\omega^2 M^2}{U^2} + \frac{2M^2 \omega \alpha}{U} - (1 - M^2) \alpha^2 \right] \Phi = 0 \quad (3)$$

The boundary condition on the solid wall (at $x = \pm H/2$ and $y = \pm H/2$) is given as

$$\frac{\partial \Phi}{\partial n} = 0 \quad (4)$$

where n is the outward normal to the boundary.

The following procedure to derive the resonance condition is repeated from Ref. 6 for easy understanding of resonance phenomena. Equation (3) can be written as

$$\Phi_{xx} + \Phi_{yy} + \Lambda^2 \Phi = 0 \quad (5)$$

Equation (5) with the boundary condition of Eq. (4) has a nontrivial solution if Λ has one of the eigenvalues Λ_n

($n = 1, 2, \dots$)

$$\Lambda_n^2 = \frac{\omega^2 M^2}{U^2} + \frac{2M^2 \omega \alpha}{U} - (1 - M^2) \alpha^2 \quad (6)$$

Rearranging this equation, we get

$$\beta^2 \alpha^2 - \frac{2M^2 \omega}{U} \alpha - \left(\frac{\omega^2 M^2}{U^2} - \Lambda_n^2 \right) = 0 \quad (7)$$

Then,

$$\beta^2 \alpha = \frac{M^2 \omega}{U} \pm \left[\frac{M^2 \omega^2}{U^2} - \beta^2 \Lambda_n^2 \right]^{1/2} \quad (8)$$

When

$$\frac{M\omega}{U} \geq \beta \Lambda_n \quad (9)$$

α has real values, and Eq. (2) represents a traveling wave of constant amplitude. When

$$\frac{M\omega}{U} < \beta \Lambda_n \quad (10)$$

then α has two conjugate complex values, and Eq. (2) is no longer a traveling wave of constant amplitude.

For each eigenvalue Λ_n , the smallest value of ω for which a disturbance of Eq. (2) can have bounded amplitude is given by

$$\omega = \omega_r = (\beta/M) U \Lambda_n \quad (11)$$

For this condition, we get the following relation from Eq. (8):

$$\alpha = M^2 \omega / U \beta^2 \quad (12)$$

Substituting Eq. (12) into Eq. (3), we can obtain the following equation:

$$\Phi_{xx} + \Phi_{yy} + (\omega/a_0 \beta)^2 \Phi = 0 \quad (13)$$

When Eq. (2) is substituted, Eq. (13) is equivalent to the following equation:

$$\phi_{xx} + \phi_{yy} - (1/a_0 \beta)^2 \phi_{tt} = 0 \quad (14)$$

This is the wave equation, with the effective speed of sound

$$a_e = a_0 \beta = a_0 \sqrt{-M^2} \quad (15)$$

Perturbation pressure is computed from the following relation, consistent with Eq. (1):

$$p = -\rho \left(\frac{\partial \phi}{\partial t} + U \frac{\partial \phi}{\partial z} \right) \quad (16)$$

From Eq. (2), pressure is given by

$$p = -i\rho(\omega + \alpha U)\phi \quad (17)$$

Using Eq. (17), we can then derive the following equation from Eq. (14):

$$p_{xx} + p_{yy} + (\omega/a_e)^2 p = 0 \quad (18)$$

This is the basic equation in the test section and will be combined with the equation for the plenum chamber to obtain the resonant frequencies in a later section.

For the plenum chamber, we assume that the velocity is zero. That is, $M = U = 0$ in the plenum chamber. Then, the

perturbation potential equation, Eq. (1), for the plenum chamber becomes

$$\psi_{zz} + \psi_{xx} + \psi_{yy} - (1/a_0^2)\psi_{tt} = 0 \quad (19)$$

Solutions of Eq. (19) must be compatible with Eq. (2) on the transonic slot.⁸ Therefore, we assume a solution of the form

$$\psi = \Psi(x, y)e^{i\alpha x}e^{i\omega t} \quad (20)$$

From Eqs. (19) and (20), we get

$$\Psi_{xx} + \Psi_{yy} - [\alpha^2 - (\omega^2)/a_0^2]\Psi = 0 \quad (21)$$

Since U is assumed to be zero in the plenum chamber, the perturbation pressure in the plenum chamber is computed from the following relation:

$$p = -\rho \left(\frac{\partial \psi}{\partial t} \right) \quad (22)$$

From Eqs. (20) and (22), pressure is given by

$$p = -i\rho\omega\psi \quad (23)$$

Substituting Eq. (12) into Eq. (21), we get the following equation:

$$\Psi_{xx} + \Psi_{yy} + (K\omega/a_0\beta)^2\Psi = 0 \quad (24)$$

where

$$K^2 = \beta^2 - \frac{M^2}{\beta^2} \quad (25)$$

Subjected to Eq. (20), Eq. (24) is equivalent to the following:

$$\psi_{xx} + \psi_{yy} - (K/a_0\beta)^2\psi_{tt} = 0 \quad (26)$$

Using the relation of Eq. (23), Eq. (26) becomes

$$p_{xx} + p_{yy} + (K\omega/a_0\beta)^2p = 0 \quad (27)$$

This equation is the basic equation for the plenum chamber.

The boundary condition on the outer walls of the plenum chamber is given as

$$\psi_y = 0 \quad (28)$$

at $y = \pm(b + H/2)$. On the slot at $y = \pm H/2$, the continuity conditions should be satisfied:

$$\phi_y = \psi_y \quad (29)$$

The governing equations and boundary conditions for the test section and plenum chamber are summarized as follows. For the test section, the governing equation is

$$\nabla^2 p_1 + (\omega/a_0\beta)^2 p_1 = 0 \quad (30)$$

The boundary condition on the solid boundary is

$$\frac{\partial p_1}{\partial n} = 0 \quad (31)$$

and on the open boundary is

$$\frac{\partial p_1}{\partial n} = \rho\omega^2\xi_1 \quad (32)$$

where ξ_1 is the normal acoustic displacement and the normal is taken to be directed out of the surface.

For the plenum chamber, the governing equation is

$$\nabla^2 p_2 + (K\omega/a_0\beta)^2 p_2 = 0 \quad (33)$$

The boundary condition on the solid boundary is

$$\frac{\partial p_2}{\partial n} = 0 \quad (34)$$

and in the open boundary is

$$\frac{\partial p_2}{\partial n} = \rho\omega^2\xi_2 \quad (35)$$

On the common open boundary, the following relation is needed to satisfy the continuity:

$$\xi_1 = -\xi_2 \quad (36)$$

III. Variational Principle

Variational principles were recently applied to acoustic problems and to the interaction between acoustics and structures.⁹⁻²⁰ Gladwell^{21,22} gives the energy and complementary energy formulations of acoustic and structural vibration systems. We will use the complementary variational principle to formulate the finite-element method for the wind-tunnel resonant problem.

In the previous section, the governing equations and boundary conditions were obtained for the test section and the plenum chamber. The governing equations, Eqs. (30) and (33), are expressed in terms of pressure, and they can be obtained from the variation of an appropriate functional. The appropriate functional for the test section is written as

$$F_1 = \frac{1}{\rho\omega^2} \left[\frac{1}{2} \left(\frac{\omega}{a_0\beta} \right)^2 \int_v p_1^2 dv - \frac{1}{2} \int_v (\nabla p_1)^2 dv \right] + \int_{S_f} \xi_1 p_1 dS \quad (37)$$

where S_f is the open boundary.

----- SLOT
——— SOLID WALL

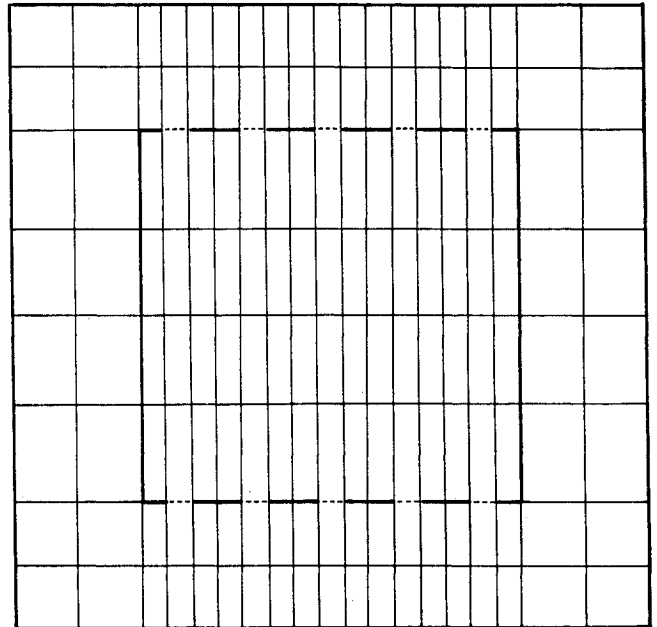


Fig. 3 Finite-element mesh for rectangular tunnel with plenum chamber (5 slots), $b = 0.333 H$.

For the plenum chamber,

$$F_2 = \frac{1}{\rho\omega^2} \left[\frac{1}{2} \left(\frac{K\omega}{a_0\beta} \right)^2 \int_v p_2^2 dv - \frac{1}{2} \int_v (\nabla p_2)^2 dv \right] + \int_{S_f} \xi_2 p_2 dS \quad (38)$$

Therefore, setting the first variation of these functionals F_1 and F_2 to zero gives the governing equations and the boundary conditions. Hence, we will use Eqs. (37) and (38) to formulate the finite-element method.

IV. Finite-Element Formulation

It was stated in the previous section that the solution of the differential equation subjected to the boundary conditions Eqs. (30-35) can be replaced by an equivalent variational principle ($\delta F_1 = 0$ and $\delta F_2 = 0$). Within each element, we can approximate the pressure distribution by row matrix $[N]_i$ of shape functions:

$$p = [N]_i \{p\}_i \quad (39)$$

Here, $\{p\}_i$ is a column vector of nodal pressure values for this i th element.

For each element, the required functionals can be obtained by substituting Eq. (39) into Eq. (37) and (38). If we define the stiffness matrix and mass matrix as $[k]_i$, $[m]_i$, respectively, we obtain

$$[k_1]_i = \int_{v_i} \left(\frac{1}{a_0\beta} \right)^2 [N]_i^T [N]_i dv \quad (40)$$

$$[k_2]_i = \int_{v_i} \left(\frac{1}{a_0\beta} \right)^2 [N]_i^T [N]_i dv \quad (41)$$

$$[m]_i = \int_{v_i} [B]_i^T [B]_i dv \quad (42)$$

$$[B]_i = \left\{ \begin{array}{c} \frac{\partial}{\partial x} \\ \frac{\partial}{\partial y} \\ \frac{\partial}{\partial z} \end{array} \right\} [N]_i \quad (43)$$

and the column vector $\{f\}_i$ on the slot is defined as

$$\{f\}_i = \int_{S_f} [N]_i^T dS \quad (44)$$

Therefore, for each element, we can get the following functionals. For the test section,

$$F_{1i} = (1/2\rho\omega^2) (\omega^2 \{p_1\}_i^T [k_1]_i \{p_1\}_i - \{p_1\}_i^T [m]_i \{p_1\}_i) + \xi_1 \{p_1\}_i^T \{f\}_i \quad (45)$$

For the plenum chamber,

$$F_{2i} = (1/2\rho\omega^2) (\omega^2 \{p_2\}_i^T [k_2]_i \{p_2\}_i - \{p_2\}_i^T [m]_i \{p_2\}_i) + \xi_2 \{p_2\}_i^T \{f\}_i \quad (46)$$

The first variation of Eqs. (45) and (46) gives the following eigenvalue problems for subvolume v_i . For the test section,

$$[m]_i \{p_1\}_i - \omega^2 [k_1]_i \{p_1\}_i - \rho\omega^2 \xi_1 \{f\}_i = \{0\} \quad (47)$$

For the plenum chamber,

$$[m]_i \{p_2\}_i - \omega^2 [k_2]_i \{p_2\}_i - \rho\omega^2 \xi_2 \{f\}_i = \{0\} \quad (48)$$

On the slot, the test section and the plenum chamber have a common open boundary on which $\xi_1 = -\xi_2$. Therefore, if we assemble the whole element, we can get the eigenvalue problem for the complete system:

$$([M] - \omega^2 [K]) \{p\} = \{0\} \quad (49)$$

For this analysis, the isoparametric finite-element is more effective.²³ Two-dimensional four-node elements are used to calculate element mass and stiffness matrices.

V. Results and Discussion

A. Rectangular Wind Tunnel

Let us consider the rectangular wind-tunnel cross section with five slots on the floor and ceiling as shown in Fig. 3. The plenum chamber surrounding the test section is rectangular in shape and has depth b . The slot open ratio is 18.0% in this case. First, we choose the wind-tunnel height as 102 mm to allow comparison with Mabey's results. The results are given in Fig. 4, in which the total number of elements used is 152, of which 60 elements are used in the test section. The trends vs Mach number are similar to Mabey's results. Although Mabey's result, which was obtained by using an averaged homogeneous boundary condition on the slots, agrees well with experimental test results, the finite-element method gives better prediction of resonant frequency.

As a second problem, we will consider the rectangular wind-tunnel cross section with one slot on the floor and ceiling as shown in Fig. 5. The plenum chamber surrounding the test section is again rectangular in shape. The slot open ratio is 33.3% in this case. The wind-tunnel height is again 102 mm. The results are given in Fig. 6, in which the total number of elements used is 45, of which 9 elements are used in the test section. The solid curve represents the resonant frequency for the slot-closed condition. The dashed curve was obtained by applying zero pressure on the slot boundary and corresponds to the resonant frequency obtained by the previous investigators²⁴ for the slot-open condition. However, this value

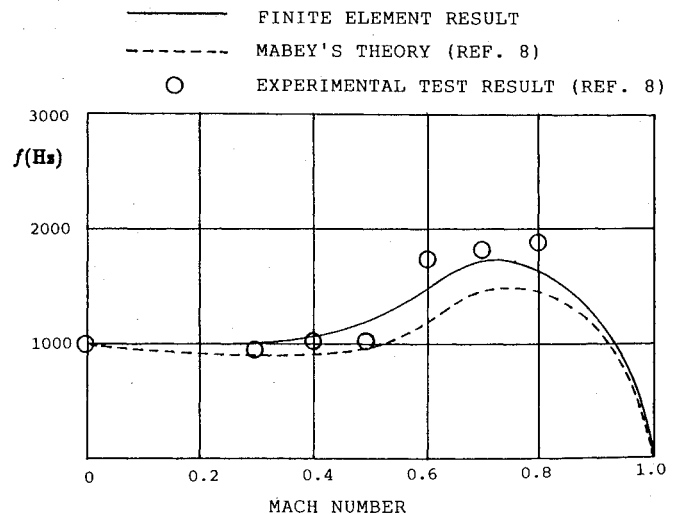


Fig. 4 Resonant frequency for rectangular tunnel with plenum chamber (5 slots), $b = 0.333 H$.

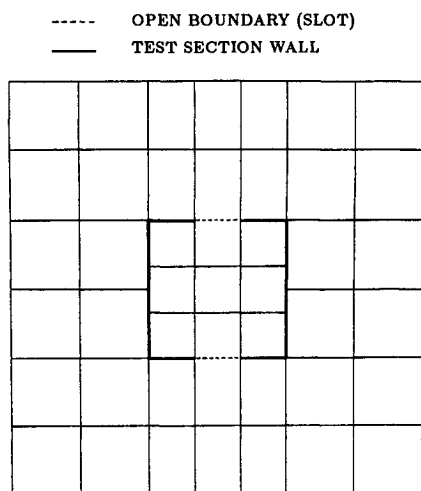


Fig. 5 Finite-element mesh for rectangular tunnel with plenum chamber (1 slot).

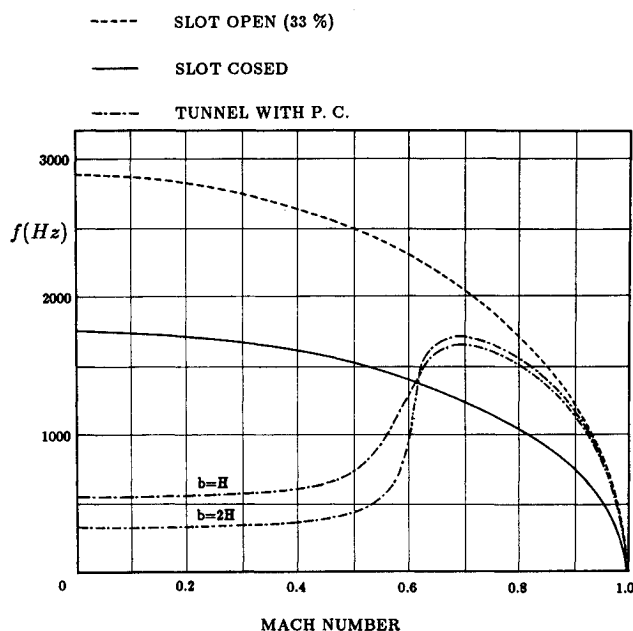


Fig. 6 Resonant frequency for rectangular tunnel with plenum chamber (1 slot).

is in considerable error when the Mach number is less than 0.618, since the plenum chamber effect on the resonance is not considered. For this analysis, two different depths of plenum chamber were considered. The trends vs Mach number are similar to the previous ones. When the Mach number is smaller than 0.618, the resonance frequency is smaller than that of the closed tunnel, whereas when the Mach number is greater than 0.618, the resonance frequency is greater than that of the closed tunnel. As the plenum chamber depth increases, the resonance frequency decreases when the Mach number is less than 0.618. The surprising change in the character of the solutions at $M=0.618$ may be explained by acoustic theory. Mabey used acoustic ray theory²⁵ to explain these characteristics. The main characteristic is that the sound wave of the test section does not enter the plenum chamber when the Mach number is greater than 0.618. Especially when $M=0.618$, the resonance frequency would be influenced by neither the open ratio nor the depth of the plenum chamber.

Another explanation is plausible, however. In the plenum chamber, the governing equation is Eq. (26). When $M=0.618$, $K^2=0$, and when M is greater than 0.618, K^2 is less than zero.

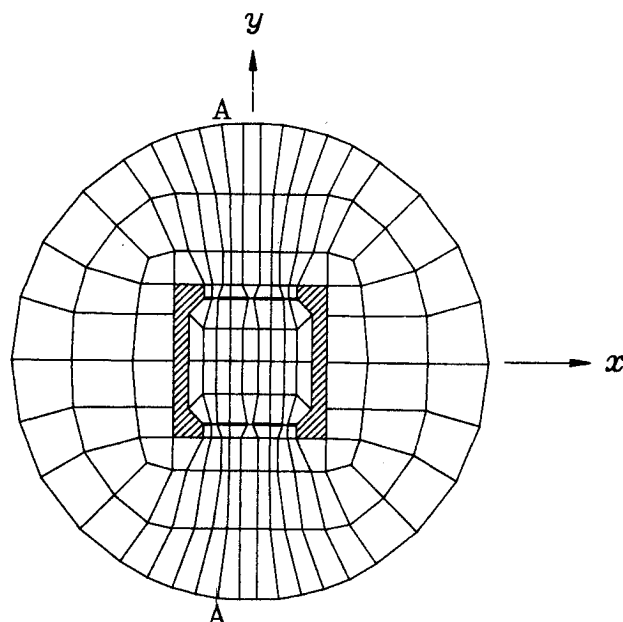


Fig. 7 Finite-element mesh for NASA Langley 16x16-ft TDT with plenum chamber.

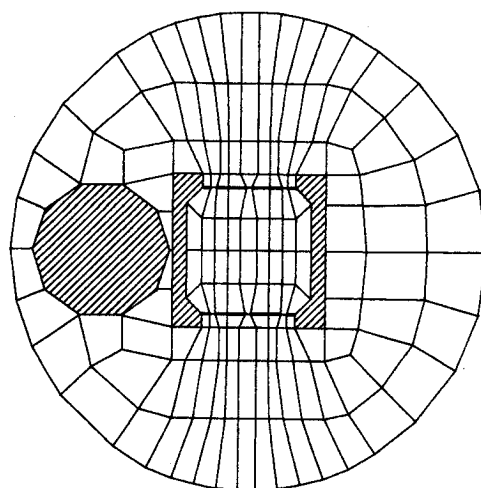


Fig. 8 Finite-element mesh for NASA Langley 16x16-ft TDT with control room in plenum chamber.

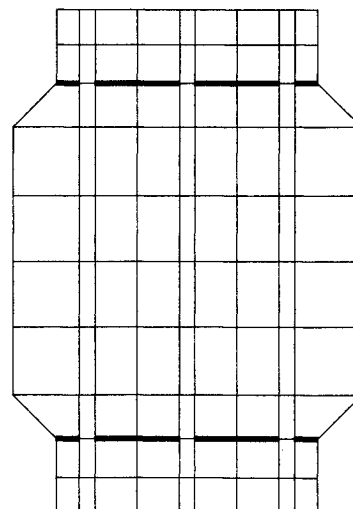


Fig. 9 Finite-element mesh for NASA Langley 16x16-ft TDT with shallow plenum chamber.

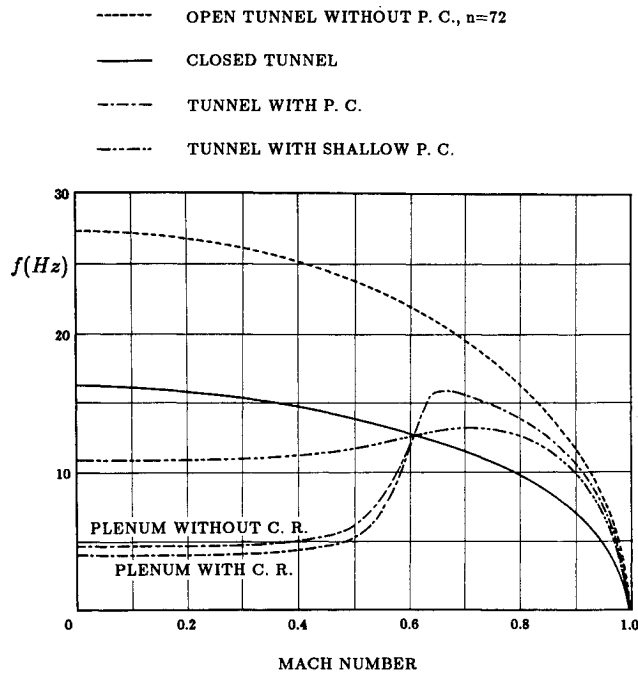


Fig. 10 Resonant frequency for NASA Langley 16×16-ft transonic dynamic tunnel.

Therefore, when M is greater than or equal to 0.618, Eq. (26) is no longer the wave equation, and the sound wave of the test section cannot propagate into the plenum chamber. However, when M is less than 0.618, K^2 is greater than zero, and Eq. (26) is the wave equation. In the test section, the governing equation, Eq. (14), is always the wave equation when the Mach number is less than 1. Therefore, the resonance characteristics of the wind tunnel with the plenum chamber will change according to whether the Mach number is greater or less than 0.618.

B. NASA Langley 16 × 16-ft Transonic Dynamics Tunnel

The NASA Langley Transonic Dynamics Tunnel (TDT) has a 16×16 ft octagonal test section surrounded by a plenum chamber whose diameter is 60 ft. The slot open ratio is 4.2%. The test medium is Freon gas, and its speed of sound is 498.7 ft/s. Figure 7 shows the finite-element mesh used to analyze the effect of the plenum chamber. Figure 8 represents the finite-element mesh used to analyze the effect of the control room in the plenum chamber. The finite-element mesh used to study the effect of the shallow plenum is given in Fig. 9.

The finite-element results are given in Fig. 10, and the resonance characters are similar to those of the rectangular tunnel. Here again $M=0.618$ is the interesting Mach number. The effect of the control room in the plenum chamber is very small, as shown in Fig. 10.

The mode shapes of the vertical vibration mode of the NASA Langley TDT are given in Fig. 11. Along the y axis, the pressure is continuous through the slot. Along section A-A in Fig. 7, the pressure is discontinuous across the solid wall, and $\partial p / \partial n$ is zero at the solid wall. When $M=0.5$, the pressure in the test section can propagate to the plenum chamber, and the pressure in the plenum chamber can also propagate into the test section. When $M=0.7$, the pressure in the plenum chamber becomes zero as the distance from the test section becomes large, and this pressure cannot propagate into the plenum chamber. Only the plenum chamber pressure near the slot is affected by the test section. Therefore, when M is greater than 0.618, the plenum chamber effect is small, whereas when M is less than 0.618, the plenum chamber effect is large.

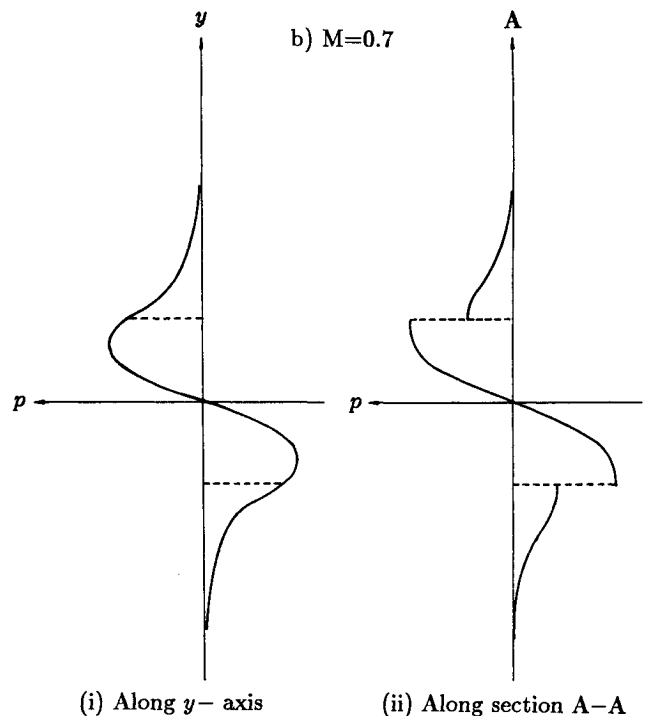
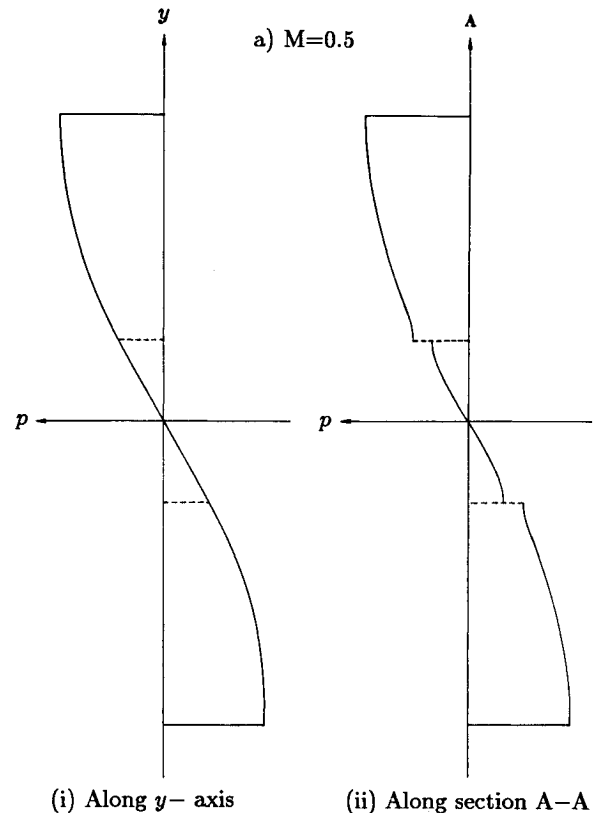


Fig. 11 Vertical vibration mode shape of NASA Langley TDT.

Acknowledgments

This research was performed under NASA Grant NGL-05-020-243. The author wishes to thank Professor Holt Ashley for his valuable discussions.

References

- Runyan, H.L., Woolston, D.S., and Rainey, A.G., "Theoretical and Experimental Investigation of the Effect of Tunnel Walls on the

Forces on an Oscillating Airfoil in Two-Dimensional Subsonic Compressible Flow," NACA Rept. 1262, 1956.

²Widmayer, E., Clevenson, S.A., and Leadbetter, S.A., "Some Measurements of Aerodynamic Forces and Moments at Subsonic Speeds on a Rectangular Wing of Aspect Ratio 2 Oscillating About the Midchord," NACA TN-4240, 1958.

³Clevenson, S.A. and Widmayer, E., "Experimental Measurements of Forces and Moments of a Two-Dimensional Oscillating Wing at Subsonic Speeds," NACA TN-3686, 1956.

⁴Runyan, H.L. and Watkins, C.E., "Considerations on the Effect of Wind-Tunnel Walls on Oscillating Air Forces for Two-Dimensional Subsonic Compressible Flow," NACA Rept. 1150, 1953.

⁵Jones, W.P., "Wind-Tunnel Wall Interference Effects on Oscillating Aerofoils in Subsonic Flow," Aeronautical Research Council, Repts. and Memoranda 2943, 1953.

⁶Acum, W.E.A., "A Simplified Approach to the Phenomenon of Wind Tunnel Resonance," Aeronautical Research Council, Repts. and Memoranda 3371, 1962.

⁷Acum, W.E.A., "Interference Effects in Unsteady Experiments," *Subsonic Wind Tunnel Wall Corrections*, AGARDograph 109, 1966, Chap. 4.

⁸Mabey, D.G., "The Resonance Frequencies of Ventilated Wind Tunnels," Aeronautical Research Council, Repts. and Memoranda 3841, 1978.

⁹Gladwell, G.M.L., "A Finite Element Method for Acoustics," *Proceedings of the Fifth International Congress on Acoustics*, Paper L.33, Liege, Belgium, Sept. 1965.

¹⁰Craggs, A., "The Transient Response of a Coupled Plate Acoustic System Using Plate and Acoustic Finite Elements," *Journal of Sound and Vibration*, Vol. 15, April 1971, pp. 509-528.

¹¹Craggs, A., "The Use of Simple Three-Dimensional Acoustic Finite Elements for Determining the Natural Modes and Frequencies of Complex Shaped Enclosures," *Journal of Sound and Vibration*, Vol. 23, No. 3, Aug. 1972, pp. 331-339.

¹²Craggs, A., "An Acoustic Finite Element Approach for Studying Boundary Flexibility and Sound Transmission Between Irregular Enclosures," *Journal of Sound and Vibration*, Vol. 30, No. 3, Oct. 1973, pp. 343-357.

¹³Herting, D.N., Joseph, J.A., Kuusinen, L.R., and MacNeal, R.H., "Acoustic Analysis of Solid Rocket Motor Cavities by a Finite

Element Method," NASA TM X-2378, 1971, pp. 285-324.

¹⁴Petyt, M., Lea, J., and Koopmann, G.H., "A Finite Element Method for Determining the Acoustic Modes of Irregular Shaped Cavities," *Journal of Sound and Vibration*, Vol. 45, April 1976, pp. 495-502.

¹⁵Shuku, T. and Ishihara, K., "The Analysis of the Acoustic Field in Irregularly Shaped Rooms by the Finite Element Method," *Journal of Sound and Vibration*, Vol. 29, No. 1, July 1973, pp. 67-76.

¹⁶Young, C.J. and Crocker, M.J., "Prediction of Transmission Loss in Mufflers by the Finite Element Method," *Journal of the Acoustical Society of America*, Vol. 57, Jan. 1975, pp. 144-148.

¹⁷Ross, D.F., "A Finite Element Analysis of Parallel-Coupled Acoustic Systems Using Subsystems," *Journal of Sound and Vibration*, Vol. 69, No. 4, 1980, pp. 509-518.

¹⁸Young, C.J., "Acoustic Analysis of Mufflers for Engine Exhaust Systems," Ph.D. Dissertation, Purdue Univ., West Lafayette, IN, 1973.

¹⁹Unruh, J.F., "Finite Element Subvolume Technique for Structural-Borne Interior Noise Prediction," *Journal of Aircraft*, Vol. 17, June 1980, pp. 434-441.

²⁰Unruh, J.F., "Structural-Borne Noise Prediction for a Single-Engine General Aviation Aircraft," *Journal of Aircraft*, Vol. 18, Aug. 1981, pp. 687-694.

²¹Gladwell, G.M.L. and Zimmerman, G., "On Energy and Complementary Energy Formulations of Acoustic and Structural Vibration Problems," *Journal of Sound and Vibration*, Vol. 3, No. 3, May 1966, pp. 233-241.

²²Gladwell, G.M.L., "A Variational Formulation of Damped Acousto-Structural Vibration Problems," *Journal of Sound and Vibration*, Vol. 4, No. 2, Sept. 1966, pp. 172-186.

²³Bathe, K.-J. and Wilson, E.L., *Numerical Methods in Finite Element Analysis*, Prentice-Hall, Englewood Cliffs, NJ, 1976.

²⁴Davis, D.D. and Moore, D., "Analytical Study of Blockage- and Lift-Interference Corrections for Slotted Tunnels Obtained by the Substitution of an Equivalent Homogeneous Boundary for the Discrete Slots," NACA RM L53E07b, June 1953.

²⁵Morse, P.M. and Ingard, K.U., "Acoustics in Moving Media," *Theoretical Acoustics*, McGraw-Hill, New York, 1968, Chap. 11.

Recommended Reading from the AIAA Progress in Astronautics and Aeronautics Series . . .



Thermophysical Aspects of Re-Entry Flows

Carl D. Scott and James N. Moss, editors

Covers recent progress in the following areas of re-entry research: low-density phenomena at hypersonic flow conditions, high-temperature kinetics and transport properties, aerothermal ground simulation and measurements, and numerical simulations of hypersonic flows. Experimental work is reviewed and computational results of investigations are discussed. The book presents the beginnings of a concerted effort to provide a new, reliable, and comprehensive database for chemical and physical properties of high-temperature, nonequilibrium air. Qualitative and selected quantitative results are presented for flow configurations. A major contribution is the demonstration that upwind differencing methods can accurately predict heat transfer.

TO ORDER: Write AIAA Order Department,
370 L'Enfant Promenade, S.W., Washington, DC 20024

Please include postage and handling fee of \$4.50 with all orders.
California and D.C. residents must add 6% sales tax. All foreign
orders must be prepaid. Please allow 4-6 weeks for delivery.
Prices are subject to change without notice.

1986 626 pp., illus. Hardback
ISBN 0-930403-10-X
AIAA Members \$59.95
Nonmembers \$84.95
Order Number V-103